Bulletin of Earthquake Engineering (2019) 17:6061–6078
https://doi.org/10.1007/s10518-019-00688-z

ORIGINAL RESEARCH

A low-cycle fatigue approach to predicting shear strength degradation in RC joints subjected to seismic actions

Carmine Lima[1] · **Enzo Martinelli**[1]

Received: 26 March 2018 / Accepted: 18 July 2019 / Published online: 22 July 2019

Abstract
Reinforced concrete (RC) structures realised in earthquake-prone regions are exposed to seismic shakings that may result in significant damage and even lead them to collapse. As well known, high stress concentration occurs at the end of both beams and columns of RC frames, making those members extremely prone to damage. Moreover, beam-to-column joints are particularly sensitive to brittle failure, especially in the cases of unreinforced and unconfined joints. This paper investigates the cyclic response of RC beam-to-column joints. Specifically, it is intended at demonstrating that the decay in shear strength due to cyclic actions can be interpreted in the light of the well-known low-cycle fatigue approach. To do so, cyclic experimental tests on RC joints reported in the scientific literature are collected and analysed. The obtained results show that the parameters governing the shear strength degradation are clearly influenced by both the layout of the RC joints and their actual design criteria. This finding highlights that low-cycle fatigue curves can be considered for describing the decay in shear strength due to cyclic actions; however, further well-documented experimental results are needed to completely identify the relationship between the relevant properties of the RC joint and the resulting low-cycle fatigue curve.

Keywords Joints · Reinforced concrete · Existing structures · Low-cycle fatigue · Strength degradation · Cyclic response

1 Introduction

Reinforced Concrete (RC) structures realised in ’60s and ‘70s of the past century are very common, both in Italy and in the whole Mediterranean area. They are widely used for public buildings, such as school, hospitals and administrative institutions (ISTAT 2001), and, then, they should guarantee high seismic performance objectives (M.II.TT. 2008; CEN 2004). However, these structures were often designed according to old codes which were

✉ Enzo Martinelli
e.martinelli@unisa.it

Carmine Lima
clima@unisa.it

[1] Department of Civil Engineering, University of Salerno, Via Giovanni Paolo II, 132, 84084 Fisciano, SA, Italy

not inspired to the modern concepts of performance-based seismic design criteria (Paulay and Priestley 1992). Therefore, they do not generally meet the safety standards required by the current codes of standards and, hence, they are generally characterised by significant levels of seismic vulnerability (Faella et al. 2006).

The observations of damage occurred during recent seismic events highlight the aforementioned critical aspects in the behaviour of existing RC frames. Specifically, they point out that the response of beam-to-column joints hugely affects their overall seismic behaviour of RC frame structures (Verderame et al. 2009).

Although several capacity models are currently available in the scientific literature for evaluating the capacity of RC members (fib 2003), they are not sufficiently accurate for beam-to-column joints (Lima 2012). In fact, these models for beam-to-column joints are based on analytical or semi-analytical formulations, either derived from mechanical considerations or empirically calibrated on experimental results (Adibi et al. 2018). Although they aim at evaluating the shear strength of RC joints, they cannot reproduce the strength and stiffness degradation induced by the cyclic nature of seismic actions, although this phenomenon is clearly highlighted by the available experimental results (Melo et al. 2015). Moreover, the same models are affected by significant levels of variability in terms of shear strength, as a result of both the different theoretical assumptions on which they are based and the variable parametric fields explored by the Authors who originally calibrated and proposed them (Lima et al. 2012a, b).

This paper aims to provide an original contribution about how to simulate shear strength degradation due to the cyclic actions in beam-to-column joints of RC frames. Specifically, the interpretation of the aforementioned strength degradation is approached by means of the low-cycle fatigue theory (Bathias and Pineau 2010), which is intended as an extension to the inelastic case of the elastic fatigue theory (high-cycle fatigue) (Palmgren 1924; Miner 1945). Therefore, Sect. 2 outlines the fundamental aspects of the low-cycle fatigue theory, which is, then, employed in Sect. 3 for determining the parameters of low-cycle fatigue curves for both interior and exterior RC joints, on the bases of a database of experimental results collected from the scientific literature. The outcome of this preliminary calibration is proposed in Sect. 4: the influence of geometric layout and design criteria (considering unreinforced, reinforced and EC8-compliant joints) clearly emerges in terms of slope of the corresponding low-cycle fatigue curves identified for the RC joints under consideration.

Finally, it is worth highlighting that, far for providing the final relationships capable to predict the low-cycle fatigue curve based on the properties of RC joints under consideration, the present paper aims at demonstrating that low-cycle fatigue is a promising approach to predicting the decay of shear strength in RC joints subjected to cyclic actions. A wider database of well-documented cyclic tests would be eventually needed to unveil the actual relationship between the low-cycle fatigue curve and the relevant properties of the RC joint under consideration.

2 Outline of the low-cycle fatigue theory

Experimental tests on RC joints subjected to under cyclic actions exhibit a degradation in terms of both strength and stiffness (Melo et al. 2015). Theoretically, this progressive reduction in strength (schematically depicted in Fig. 1) can be interpreted within the general framework of low-cycle fatigue theory (Bathias and Pineau 2010), which is an extension of the

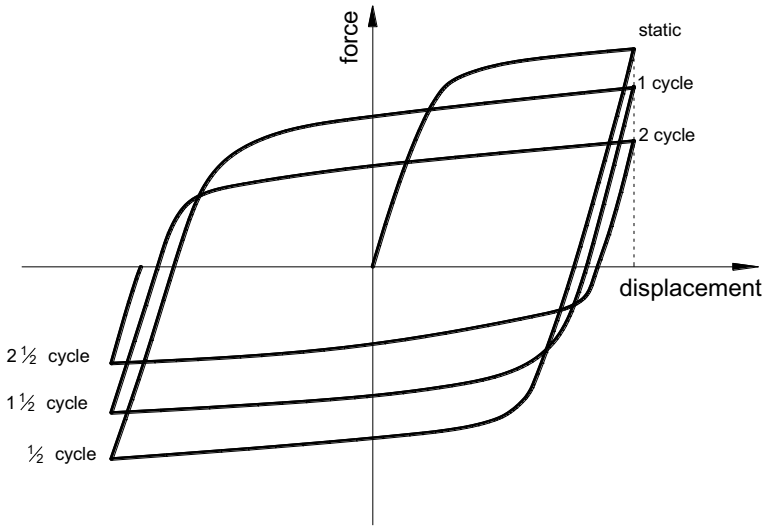

Fig. 1 Strength degradation of a generic structural component under cyclic displacements with constant amplitude

theory attributed to Palmgren (1924) and Miner (1945) for describing the failure of mechanical components subjected to a high number of cyclic excitations, though within the elastic range.

As a matter of fact, the concept of Low-Cycle Fatigue is extensively used in earthquake engineering and generally aims at evaluating the number and amplitude of cycles leading to failure of a structural component under cyclic actions (Mander et al. 1994). Specifically, a functional D can be generally defined in order to represent the cumulated damage due to the cyclic actions. According to the assumptions of Palmgreen-Miner, the damage D induced by a history of n_1 cycles with constant amplitude V_1 can be expressed as follows:

$$D = \frac{n_1}{N_1} \tag{1}$$

where N_1 is the number of cycles leading to failure under the same amplitude V_1.

In the general cases of cycles characterised by variable amplitudes (Fig. 2), the expression of the damage functional D defined in Eq. (1) can be generalised as follows (Miner 1945):

$$D = \frac{n_i}{N_i} + \frac{n_2}{N_2} + \frac{n_3}{N_3} \cdots \tag{2}$$

where n_i is the actual number of cycles with amplitude V_i and N_i is the corresponding number of equal amplitude cycles leading to failure. In principle, in this case failure is expected to occur (conventionally) when the functional D is equal to the unit:

$$D = \sum_{i}^{k} \frac{n_i}{N_i} = 1. \tag{3}$$

in which k represents the number of cycle groups of equal amplitude.

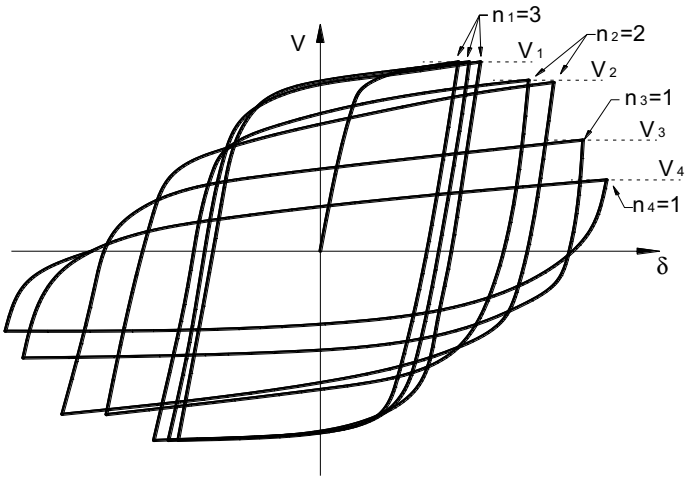

Fig. 2 Hysteretic response under cyclic actions with variable amplitude

Four seismic performance levels (i.e., fully operational, immediate occupancy, life safety, and collapse prevention) are generally considered to describe the expected performance of buildings, or alternatively, the expected damage, and economic loss. Therefore, according to the scientific literature (Cosenza and Manfredi 2000) structural collapse is supposed to occur as $D > 1$, whereas structural damage is still reparable for $D < 0.5$. In the case of $0.5 < D < 1.0$, collapse does not occur, but the building (or the structural member under consideration) is not reparable. Moreover, for $D < 0.2$ damage is supposed to be negligible.

Jiang et al. (2011) suggested specific values of D related to the Limit States generally considered in seismic analysis of structures. In particular, damage index D less than 0.05 implies fully operational capabilities; from 0.05 to 0.15, immediate occupancy capability; from 0.15 to 0.45, life safety; and from 0.45 to 1.0, incipient collapse.

Based on a generalised Palmgren–Miner rule (Hashin 1979), the amplitude V_i leading to failure of the element subjected to a defined number of cycles N_i is related to the strength V_{mon} under monotonic action as follows:

$$\log\left(V_i\right) = \log(V_{mon}) - \frac{1}{m}\log(N_i). \tag{4}$$

where m is a parameter defining the degradation effect.

The Eq. (4) assumes a linear relationship (in a log–log plane) between ultimate shear strength and available number of cycles up to failure (Fig. 3). Specifically, the (logarithm of) strength decreases linearly with the (logarithm of) the number of cycles.

If the parameter m and the monotonic strength V_{mon} are known, the number of cycles N_i needed for inducing failure due to an action of given amplitude $V_i < V_{mon}$ can be evaluated by solving Eq. (4) with respect to N_i:

$$N_i = \left(\frac{V_i}{V_{mon}}\right)^{-m}. \tag{5}$$

In case of cyclic protocols characterised by variable amplitudes, the following relationship can be determined by replacing Eq. (5) in Eq. (2) and fixing the limit condition dictated by Eq. (3):

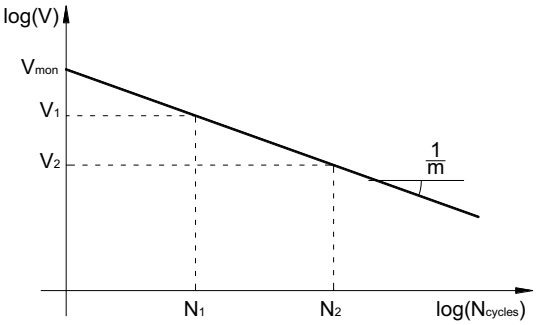

Fig. 3 Relationship between shear strength and number of cycles needed for acting joint failure

$$\sum_{i=1}^{k} \frac{n_i}{\left(\frac{V_i}{V_{mon}}\right)^{-m}} = 1, \tag{6}$$

where k, representing the number of cycle groups of equal amplitude, can be recognised throughout the load history up to the specimen failure.

Referring to RC joints analysed in this paper, Eq. (6) includes 2 unknown terms:

- the parameter m;
- the shear strength under monotonic loads V_{mon}.

Therefore, at least two nominally identical specimens tested under both monotonic and cyclic loads would be needed to identify the aforementioned low-cycle fatigue curve: V_{mon} could be determined from the former, whereas the cyclic test performed with action $V_i < V_{mon}$ could be considered for estimating the corresponding number of m from Eq. (6) with $k = 1$. This condition is not achieved for any tests in the selected database, which only collects cyclic tests. Hence, an alternative estimation of the monotonic shear strength is required for deriving the fatigue curve.

Based on the comprehensive assessment and comparison proposed by Lima et al. (2012a), the model by Kim et al. (2009) exhibited the highest accuracy and reliability among those considered in a comparative study (Lima et al. 2012b): hence, that model is employed herein for determining V_{mon} based on the geometric and mechanical properties available for each RC joints mentioned within the database.

Therefore, once the monotonic shear strength is estimated, Eq. (6) can be solved for determining the parameter m, as described in the following Sect. 3.

3 Evaluation of the low-cycle fatigue curves

3.1 Shear strength under monotonic actions

As already mentioned in Sect. 2, the empirical model by Kim et al. (2009) is employed hereafter for estimating the monotonic shear strength V_{mon} of RC joints under consideration which were tested under cyclic conditions. It was originally developed on the basis of a wide database collecting experimental tests performed on both interior and exterior joint. A first version of the model (Kim et al. 2007) took into account joints with shear reinforcement only, while

shear strength equal to zero was provided for unreinforced joints. Two years later, Kim et al. (2009) recalibrated the model on the basis of a database wider than the one used in 2007 including unreinforced joints in order to extend the formulation to the case of joints without stirrups.

According to this proposal, the shear strength of reinforced concrete joints can be evaluated by multiplying the specific shear strength v_{jh} for the geometric dimension of the joint panel:

$$V_{jh} = v_{jh} \cdot b_j \cdot h_c, \tag{7}$$

in which h_c is the height of the column cross section and b_j is the effective width of the joint panel which is provided by the following relationship:

$$b_j = \min\left(b_c\,; \frac{b_c + b_b}{2}\right), \tag{8}$$

where b_c and b_b are the width of the column and the beam, respectively.

The joint specific shear strength v_{jh} is evaluated as follows:

$$v_{jh} = \alpha_t \cdot \beta_t \cdot \eta_t \cdot \lambda_t \cdot (JI)^{0.15} \cdot (BI)^{0.30} \cdot f_c^{0.75}, \tag{9}$$

in which α_t is a parameter used for describing the in-plane geometry of the beam-to-column joint: it is assumed equal to the unit for interior joints, 0.7 for exterior ones and 0.4 for knee connections (characterised by the absence of the top column). Moreover, the β_t coefficient describes the out-of-plane geometry and is equal to 1.0 for joints without transversal beams or 1.18 otherwise, while $\lambda_t = 1.31$ is fixed by the authors (Kim et al. 2009) in order to correlate values of shear strength obtained through Eq. (9) to the ones observed in experimental tests collected in the considered experimental database. The concrete compressive strength is denoted as f_c, while other quantities of Eq. (9) are defined in the following:

$$\eta_t = \left(1 - \frac{e_b}{b_c}\right)^{0.67}, \tag{10}$$

$$BI = \frac{\rho_b \cdot f_{yb}}{f_c}, \tag{11}$$

$$JI = \frac{\rho_j \cdot f_{yj}}{f_c} \geq 0.0139, \tag{12}$$

where f_{yb} and f_{yj} denote the yield stress of longitudinal bars in the beams and horizontal stirrups within the joint, respectively. The limitation above 0.0139 to JI was introduced later with the aim to cover the case of unreinforced joints (Kim et al. 2009).

The beam reinforcement ratio ρ_b and the volumetric joint transverse reinforcement ratio ρ_j introduced in Eqs. (11) and (12) are defined as follows:

$$\rho_b = \frac{A_{sb,\mathrm{sup}} + A_{sb,\mathrm{inf}}}{b_b \cdot h_c}, \tag{13}$$

$$\rho_j = \frac{A_{sjh} \cdot h_c}{h_c \cdot b_c \cdot \left(h_b - 2d'\right)}, \tag{14}$$

where $A_{sb,sup}$ e $A_{sb,inf}$ are the longitudinal reinforcement at the top and bottom of the beam, respectively, A_{sjh} is the area of horizontal stirrups in the joint panel, b_c, h_c, b_b and h_b are the geometric dimensions of the cross sections of the beam and the column and d' is the thickness of the concrete which cover steel bars.

Finally, the parameter η_t [Eq. (10)] takes into account the eccentricity e_b between the beam and the column axes, while BI and JI are two parameters which consider the effects of the amounts of steel reinforcement in the beam [Eq. (11)] and the joint panel [Eq. (12)], respectively.

3.2 The experimental database

The behaviour of beam-to-column joints under cyclic loading is highly influenced by several seismic details including the amount of shear reinforcement and the anchorage of rebars in beam. The present study is based on a subset of the database collected as part of the first Author's Ph.D. Thesis (Lima 2012). The database is partitioned between interior and exterior joints and a further distinction between unreinforced and reinforced members. Test reports providing detailed information about geometric dimensions, materials and the load history are selected within the wide database of experimental tests. In particular, 24 interior joint specimens are selected and analysed, 4 of which were unreinforced and 20 were internally reinforced by stirrups (Table 1). As for exterior joints, 31 experimental tests are selected, collecting 3 and 28 tests on unreinforced and reinforced joint specimens (Table 2).

Both tables report the reference to the source article, the original identification code (ID) of each specimen and information about whether the joint is reinforced (R) or not (U): in the case of reinforced joints the tables also clarify whether the amount of steel stirrups complies or not with EC8 provisions (CEN 2004). Moreover, the observed failure mode is also mentioned in the tables, which can be either:

- Shear failure of the joint with beam and columns in the elastic range (J);
- Shear failure of the joint after formation of a plastic hinge in the beam (BJ);
- Shear failure of the joint after formation of a plastic hinge in the column (CJ).

Finally, further aspects about structural details are highlighted for each specimen and described at the bottom of both tables.

The scientific literature collects a limited number of experimental tests performed under cyclic conditions, especially about unreinforced joints. As a matter of fact, this is due to both the low displacement capacity and the significant strength degradation of such subassemblies, which makes difficult to perform tests under loading reversals.

The number of cycles and the shear force at each cycle are derived from the graphs reporting the load–displacement relationship of the specimen considered. The parameter m of each test is evaluated through [Eq. (6)]. Conventionally, failure is attained as soon as a strength decay equal to 20% is observed.

As an example, and Table 3 report the processing of experimental results of the interior joint labelled X1 tested by Durrani and Wight (1982) and described in Fig. 4.

Specifically, the sequence of operations performed for evaluating the parameters n1 and N1 needed to back-calculate the exponent m are depicted in Fig. 5. The first complete cycle n_1 ranges between 6.35 and −5.08 mm (Fig. 5) which corresponds to the shear strength $V_1 = 212.67$ kN.

Table 1 Database: reports about experimental tests on interior joints

Authors	Test ID	R-reinforced or U-unreinforced	Type of failure	Details[a]
Hakuto et al. (2000)	O1	U	J	C
Li et al. (2002)	A1	U	J	BS
	A2	U	BJ	BS
	M2	R (under-reinforced)	BJ	C
Pampanin et al. (2002)	C2	U	CJ	C
Durrani and Wight (1982)	X1	R (under-reinforced)	J	C
	X2	R (under-reinforced)	J	C
Kitayama et al. (1991)	J1	R (under-reinforced)	J	C
Kusuhara et al. (2004)	JE-0	R (under-reinforced)	J	C
	JE-55	R (under-reinforced)	J	C
	JE-55S	R (under-reinforced)	J	C
Lee et al. (2009)	J1	R (under-reinforced)	J	C
	BJ1	R (under-reinforced)	BJ	C
	BJ2	R (under-reinforced)	BJ	C
	BJ3	R (under-reinforced)	BJ	C
	B1	R (under-reinforced)	BJ	C
Leon (1990)	BCJ3	R (under-reinforced)	J	C
	BCJ4	R (under-reinforced)	BJ	C
Shin and LaFave (2004)	1	R (under-reinforced)	J	C
	2	R (under-reinforced)	J	C
Shiohara et al. (2000)	S3	R (under-reinforced)	J	C
Takaine et al. (2008)	JH1	R (under-reinforced)	BJ	C
Teng and Zhou (2003)	S1 (series1)	R (under-reinforced)	J	C
	S6 (series6)	R (under-reinforced)	J	C

[a]*C* continuous longitudinal bars in beam, *BS* beam bottom bar lap spliced within joint

After the first cycle (i = 1), Eq. (6) can be applied obtaining a value of damage D lower than the unit and dependent from the parameter m only (Table 3). The second cycle shows a shear force V_2 equal to 992.47 kN, while at the third one $V_3 = 1016.10$ kN is recorded. Also, for the second (i = 2) and third (i = 3) cycles Eq. (6) is applied and the corresponding damage is obtained as a function of the unknown parameter m. The processing operations described above are replicated until the conventional failure (strength decay equal to 20%).

Finally, the parameter m is back-calculated by solving Eq. 6: the result $m = 20.58$ is actually obtained.

3.3 Interior joints

The procedure described above at the end of Sect. 3.2 is applied to the interior joints collected in the database. Tables 4 and 5 report the *m* values determined for unreinforced and reinforced interior joints, respectively. The analysis of the experimental results shows that the mean value of the parameter m governing the low-cycle fatigue of unreinforced interior joints (Table 4) is equal to 4.88 with a corresponding value of the standard deviation $\sigma(m) = 1.28$.

Table 2 Database: reports about experimental tests on exterior joints

Authors	Test ID	R-reinforced or U-unreinforced	Type of failure	Details[a]
Karayannis et al. (2008)	A0	U	J	L
	A1	R (EC8-compliant)	BJ	L
	B1	R (under-reinforced)	BJ	L
Karayannis and Sirkelis (2008)	A1	U	J	L
	A2	U	J	L
Chalioris et al. (2008)	JB-s1	R (under-reinforced)	J	L
Chun and Kim (2004)	JC-2	R (under-reinforced)	J	L
	JM-2	R (under-reinforced)	J	H
Ehsani and Alameddine (1991)	LL11	R (under-reinforced)	BJ	L HSC
	HL11	R (under-reinforced)	BJ	L HSC
	HH14	R (under-reinforced)	BJ	L HSC
Ehsani et al. (1987)	1	R (under-reinforced)	BJ	L HSC
	2	R (under-reinforced)	BJ	L HSC
	3	R (under-reinforced)	BJ	L HSC
Ehsani and Wight (1985a, b)	1B	R (under-reinforced)	BJ	L
	2B	R (under-reinforced)	BJ	L
	3B	R (under-reinforced)	BJ	L
	5B	R (under-reinforced)	BJ	L
	6B	R (under-reinforced)	BJ	L
Lee and Ko (2007)	W0	R (EC8-compliant)	BJ	L
	W75	R (EC8-compliant)	BJ	L
	W150	R (EC8-compliant)	BJ	L
Tsonos (2007)	G1	R (under-reinforced)	J	L
Tsonos et al. (1992)	S2	R (EC8-compliant)	J	L
	S6	R (under-reinforced)	J	L
Wong and Kuang (2008)	BS-L-H1	R (under-reinforced)	J	L

[a] *L* 90° standard hook of longitudinal beam bars, *H* mechanical hook of longitudinal beam bars, *HSC* high strength concrete (55–100 MPa)

Figure 6 depicts (in grey) the low-cycle fatigue curves derived for each specimen about unreinforced interior joints. The following equation describes the low-cycle fatigue curves:

$$\frac{V}{V_{mon}} = N^{-\frac{1}{m}}. \tag{15}$$

The thick black line in Fig. 6 represents the mean curve associated to m = 4.88.

The mean value of the parameter m for reinforced interior joints is evaluated by considering only 20 cyclic tests and neglecting the two tests providing the maximum and

Table 3 Processing experimental results of X1 specimen

Cycle	No. cycle at equal amplitude—n_i	δ_i (mm)	V_i (kN)	Progressive damage functional D_i	Cumulative damage
		6.35	212.67	3.066E−15	
n_1	1	−5.08	−212.67		3.066E−15
		40.64	992.47	1.799E−01	
n_2	1	−38.1	−992.47		1.799E−01
		50.8	1016.10	2.920E−01	
n_3	1	−50.8	−1016.10		4.719E−01
		63.5	1016.10	2.920E−01	
n_4	1	−63.5	−1016.10		7.638E−01
		83.82	992.47	1.799E−01	
n_5	1	−83.82	−992.47		9.437E−01
		104.14	921.58	5.087E−02	
n_6	1	−101.6	−945.21		9.946E−01
		119.38	850.69	5.652E−03	
n_7	1	−119.38	−827.06		1.000
		134.62	756.17	3.473E−04	
n_8	1	−137.16	−708.91		1.000

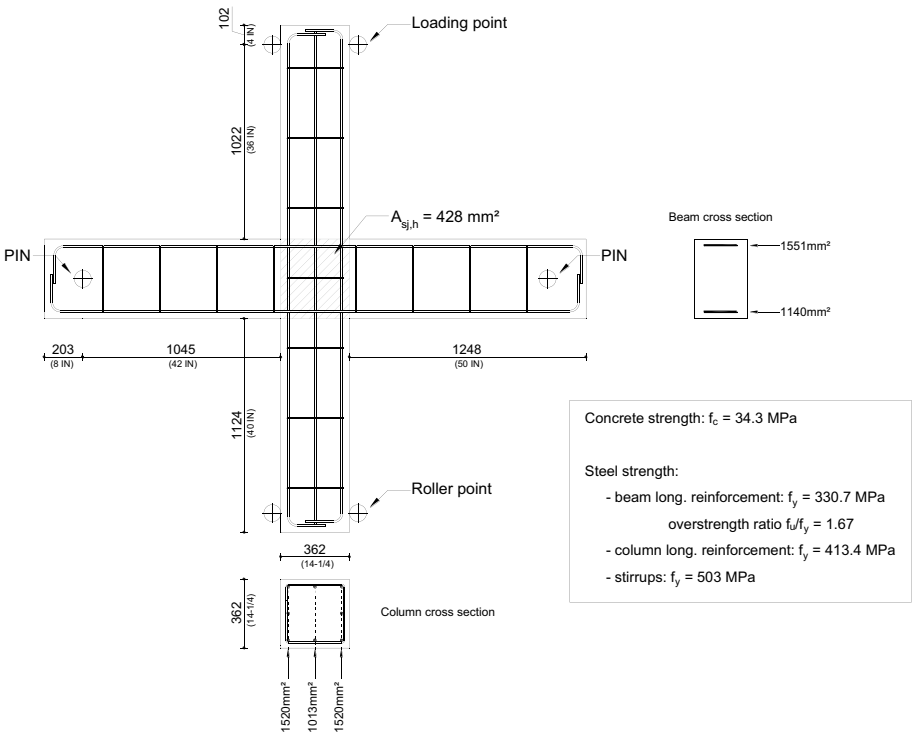

Fig. 4 Geometry and structural details of specimen X1 tested by Durrani and Wight (1982)

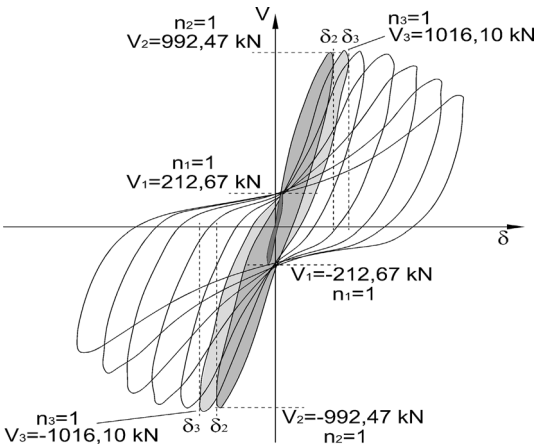

Fig. 5 Counting the number of cycles for estimating the damage parameter

Table 4 Parameter m evaluated for unreinforced interior joints

Authors	label	m
Hakuto et al. (2000)	O1	4.49
Li et al. (2002)	A1	3.28
	A2	6.22
Pampanin et al. (2002)	C2	5.50

Table 5 Parameter m evaluated for reinforced interior joints

Authors	Label	m
Li et al. (2002)	M2	3.26
Durrani and Wight (1982)	X1	20.58
	X2	10.52
Kitayama et al. (1991)	J1	4.40
Kusuhara et al. (2004)	JE-0	5.59
	JE-55	6.25
	JE-55S	5.97
Lee et al. (2009)	J1	5.16
	BJ1	5.45
	BJ2	5.43
	BJ3	7.43
	B1	8.26
Leon (1990)	BCJ3	8.67
	BCJ4	2.80
Shin and LaFave (2004)	1	5.45
	2	5.69
Shiohara et al. (2000)	S3	4.69
Takaine et al. (2008)	JH1	4.60
Teng and Zhou (2003)	S1 (series1)	6.28
	S6 (series6)	9.62

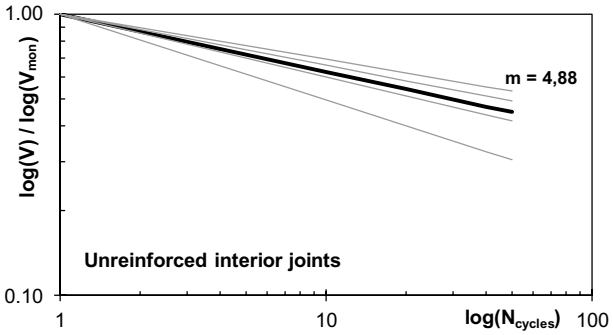

Fig. 6 Low-cycle fatigue curves determined for unreinforced interior joints

minimum values of m, respectively (Table 5). Specifically, the mean value m = 6.08 is obtained for the 18 processed tests and the corresponding standard deviation is σ(m) = 2.03.

Figure 7 shows the low-cycle fatigue curves derived from the 18 experimental tests under consideration (in grey) and the mean curve related to reinforced interior joints. It is worth observing that the average curve determined for unreinforced joints is slightly steeper than the one obtained for reinforced ones, which means that, as expected, the latter are less prone to strength degradation than the former.

3.4 Exterior joints

Tables 6 and 7 report the values of the parameter m derived from experimental tests performed on unreinforced and reinforced exterior joints, respectively.

The processing of experimental results provides a mean value of the parameter m associated to unreinforced exterior joints equal to 3.85 with a standard deviation σ(m) = 1.29. Figure 8 shows the low-cycle fatigue curves of the three unreinforced exterior joints under consideration (in grey) and the mean curve (thick line).

The mean value of m evaluated for reinforced exterior joints (Table 7) is equal to 7.58, while its standard deviation is σ(m) = 2.92.

Figure 9 depicts the low-cycle fatigue curves derived for reinforced exterior joints (in grey). The results are characterised by high value of dispersion if compared with the ones obtained for interior joints.

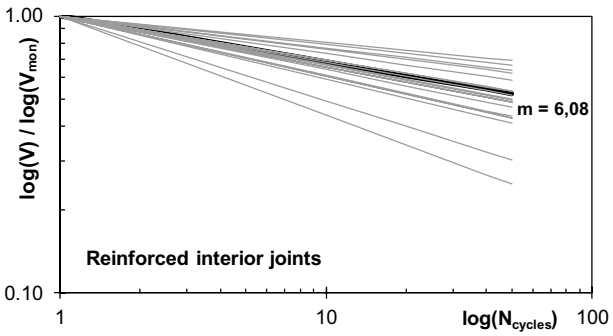

Fig. 7 Low-cycle fatigue curves determined for reinforced interior joints

Table 6 Parameter m evaluated for unreinforced exterior joints

Authors	Label	m
Karayannis et al. (2008)	A0	5.32
Karayannis and Sirkelis (2008)	A1	3.30
	A2	2.93

Table 7 Parameter m evaluated for reinforced exterior joints

Authors	Label	m
Chalioris et al. (2008)	JB-s1	4.06
Chun and Kim (2004)	JC-2	5.69
	JM-2	5.83
Ehsani and Alameddine (1991)	LL11	5.68
	HL11	5.38
	HH14	6.84
Ehsani et al. (1987)	1	8.69
	2	9.70
	3	8.21
Ehsani and Wight (1985a, b)	1B	5.48
	2B	8.17
	3B	9.10
	5B	4.02
	6B	3.37
Karayannis et al. (2008)	A1	10.43
	B1	4.05
Lee and Ko (2007)	W0	12.63
	W75	13.59
	W150	10.41
Tsonos (2007)	G1	8.02
Tsonos et al. (1992)	S2	5.49
	S6	7.39
Wong and Kuang (2008)	BS-L-H1	12.13

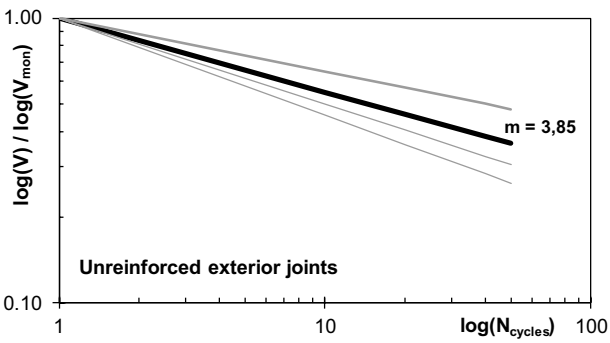

Fig. 8 Low-cycle fatigue curves evaluated for unreinforced exterior joints

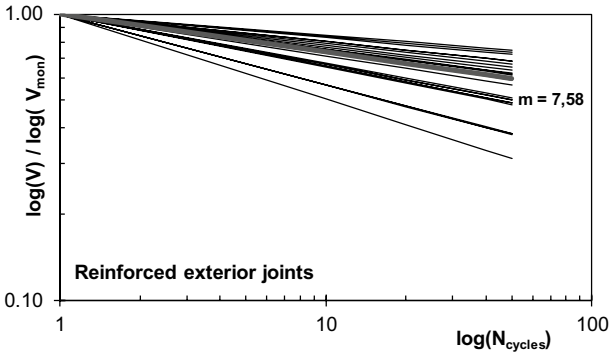

Fig. 9 Low-cycle fatigue curves determined for reinforced exterior joints

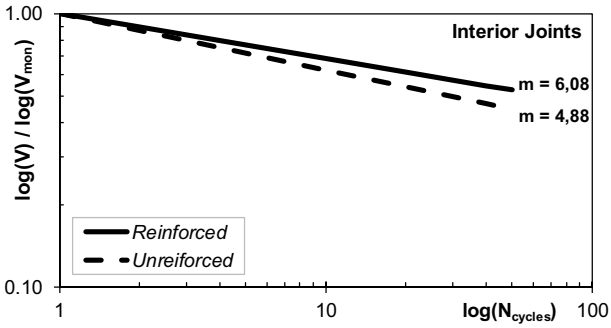

Fig. 10 Low-cycle fatigue curves for interior joints: comparison between unreinforced and reinforced ones

Finally, also for exterior joints the low-cycle fatigue curve obtained for unreinforced joints is steeper than the one for reinforced joints. In this case the difference between the two curves is slightly more pronounced than in the case of interior joints, as shear strength in the former rely more on stirrups than in the latter, which are confined by the two adjacent beams.

4 Results and comparisons

Figure 10 shows the comparison between the mean low-cycle fatigue curves obtained for both unreinforced and reinforced interior joints. Unreinforced beam-to-column joints are characterised by degradation faster than the one observed in reinforced interior connections. The standard deviations evaluated in the previous section equal to 1.28 and 2.03 for unreinforced and reinforced joints, respectively.

The comparison reported in Fig. 10 shows a limited different behaviour between unreinforced and reinforced joints demonstrating that, for interior ones, beams provide a significantly beneficial confinement effects and, consequently, the presence of horizontal stirrups within the panel zone does play a significant role in reducing the strength degradation under cyclic actions. The standard deviations evaluated in the previous section equal to 1.28 and 2.03 for unreinforced and reinforced joints, respectively.

Conversely, as it might have been expected, in exterior joints the absence of horizontal reinforcements in the panel zone leads to a significant difference in terms of damage evolution under cyclic actions (Fig. 11). This apparent difference is “measured” by two

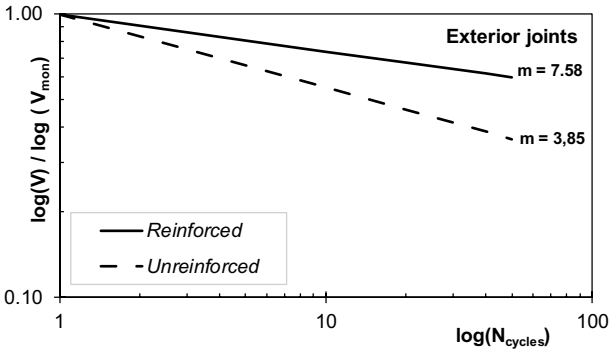

Fig. 11 Low-cycle fatigue curves for exterior joints: comparison between unreinforced and reinforced ones

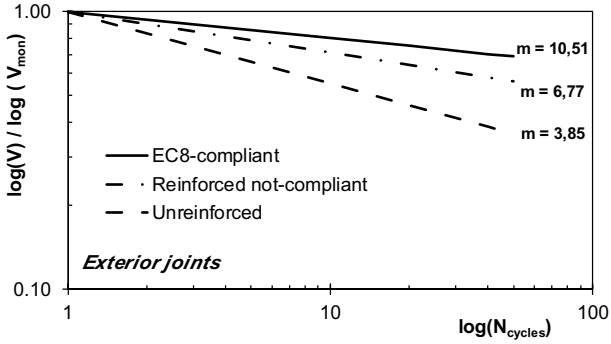

Fig. 12 Low-cycle fatigue curves for reinforced exterior joints: difference between EC8 compliant and under-designed joints

significantly different values of the average m determined for unreinforced and reinforced external RC joints. Specifically, unreinforced joints exhibit an average value of m equal 3.85 with a standard deviation $\sigma(m) = 1.29$, whereas reinforced joints lead to an average m equal to 7.58 with standard deviation $\sigma(m) = 2.92$.

Finally, Fig. 12 shows that further differences emerge in the mean fatigue curves determined for EC8-compliant and non-compliant reinforced joints (Table 2). Specifically, the slope of the fatigue curve (and, hence, the proneness to damage under cyclic actions) is lower in EC8-compliant joints ($m = 10.51$) than in reinforced and non-compliant joints ($m = 6.77$).

5 Conclusions

This study proposes an original interpretation of cyclic behaviour of RC joints. Specifically, it follows an approach based on the Theory of Low-Cycle Fatigue for interpreting the reduction in shear strength observed in experimental tests under cyclic actions. A significant number of experimental tests taken from the scientific literature have been processed with the aim to determine the number and amplitude of cycles leading them to fail in shear. More specifically, both interior and exterior joints are considered and the response of both unreinforced and reinforced joints are analysed separately. The following conclusions are worthy to be highlighted:

- the different responses observed in the experimental tests considered for interior and exterior joints, and for unreinforced and reinforced, ones is clearly caught by the proposed interpretation in terms of low-cycle fatigue curve;
- in fact, the influence of reinforcement in terms of the estimated m value is more apparent for exterior joint than for interior ones, as in the former stirrups are the only elements capable to realise a confining effect resulting in a lower strength degradation;
- furthermore, as expected, the amount of reinforcement plays a role in the resulting proneness to damage under cyclic actions: the slope of the resulting mean fatigue curves is slightly lower for EC8-compliant joints than for under designed ones.

Finally, far from proving readers with the final calibration of fatigue curves for the considered classes of joints (which would require a much wider number of well-documented experimental results), this study demonstrates that the degradation in strength of beam-to-column joints induced by cyclic actions can be regarded within the general framework of low-cycle fatigue theory. Further studies are needed to better calibrate the fatigue curves of interior and exterior joints, taking into account several relevant aspects, such as the amount and structural detailing of rebars and the properties of materials.

Acknowledgements This research has been developed as part of the DPC-ReLUIS 2010–2013 Project (Task 1.1.2).

References

Adibi M, Marefat MS, Allahvirdizadeh R (2018) Nonlinear modeling of cyclic response of RC beam-column joints reinforced by plain bars. Bull Earthq Eng 16:5529–5556

Bathias C, Pineau A (2010) Fatigue of materials and structures. Fundamentals. Wiley, Hoboken. ISBN 978-1-84821-051-6

CEN "European Committee for Standardization" (2004) Eurocode 8: design of structures for earthquake resistance—Part 1: General rules, seismic actions and rules for buildings. EN 1998-1

Chalioris CE, Favvata MJ, Karayannis CG (2008) Reinforced concrete beam-column joints with crossed-inclined bars under cyclic deformations. Earthq Eng Struct Dyn 37:881–897. https://doi.org/10.1002/eqe.793

Chun SC, Kim DY (2004) Evaluation of mechanical anchorage of reinforcement by exterior beam-column joint experiments. In: 13th world conference on earthquake engineering, August 1–6, 2004; Paper no. 0326, Vancouver

Cosenza E, Manfredi G (2000) Damage indices and damage measures. Prog Struct Mater Eng 2:50–59. https://doi.org/10.1002/(SICI)1528-2716(200001/03)2:13.3.CO;2-J

Durrani AJ, Wight JK (1982) Experimental and analytical study of internal beam-to-column connections subjected to reversed cyclic loading. Report UMEE 82R3, Department of Civil Engineering, University of Michigan, Michigan

Ehsani MR, Alameddine F (1991) Design recommendations for type 2 high-strength reinforced concrete connections. ACI Struct J 88(3):227–291

Ehsani MR, Wight JK (1985a) Effect of transverse beam and slab on behavior of reinforced concrete beam-to-column connections. ACI Struct J 82(17):188–195

Ehsani MR, Wight JK (1985b) Exterior reinforced concrete beam-to-column connections subjected to earthquake type loading. ACI Struct J 82(43):492–499

Ehsani MR, Moussa AE, Vallenilla CR (1987) Comparison of inelastic behavior of reinforced ordinary- and high-strength concrete frames. ACI Struct J 84(s17):161–169

Faella C, Martinelli E, De Santo D, Nigro E (2006) Some Remarks on the seismic assessment of RC existing buildings in Italy according to the recent codes. In: Proceedings of the 1st European conference on earthquake engineering and seismology, paper 1375, Genève

fib "Fédération International du Béton" (2003) Bulletin 24: seismic assessment and retrofit of reinforced concrete buildings. Lausanne (CH). ISBN: 978-2-88394-064-2

Hakuto S, Park P, Tanaka H (2000) Seismic load tests on interior and exterior beam-column joints with substandard reinforcing details. ACI Struct J 97(1):11–25

Hashin Z (1979) A reinterpretation of Palmgren–Miner rule for fatigue life prediction. Technical report no. 1. Department of Materials Science and Engineering, College of Engineering and Applied Science, University of Pennsylvania, Philadelphia

ISTAT "National Institute of Statistics" (2001) L'Italia in 150 anni. Sommario di statistiche storiche 1861-2010 (in Italian). RTI Poligrafica Ruggiero S.r.l.—ACM S.p.a., Avellino

Jiang HJ, Chen LZ, Chen Q (2011) Seismic damage assessment and performance levels of reinforced concrete members. Proc Eng 14:939–945. https://doi.org/10.1016/j.proeng.2011.07.118

Karayannis CG, Sirkelis GM (2008) Strengthening and rehabilitation of RC beam-column joints using carbon-FRP jacketing and epoxy resin injection. Earthq Eng Struct Dynam 37:769–790. https://doi.org/10.1002/eqe.785

Karayannis CG, Chalioris CE, Sirkelis GM (2008) Local retrofit of exterior RC beam-column joints using thin RC jackets—an experimental study. Earthq Eng Struct Dynam 37:727–746. https://doi.org/10.1002/eqe.783

Kim J, LaFave JM, Song J (2007) A new statistical approach for joint shear strength determination of RC beam-column connections subjected to lateral earthquake loading. Struct Eng Mech 27(4):439–456

Kim J, LaFave JM, Song J (2009) Joint shear behaviour of reinforced concrete beam-column connections. Mag Concrete Res 61(2):119–132. https://doi.org/10.1680/macr.2008.00068

Kitayama K, Otani S, Aoyama H (1991) Development of design criteria for RC interior beam-column joints. In: James OJ (ed) Published in ACI SP123 design of beam-columns joints for seismic resistance. American Concrete Institute, Michigan, pp 97–123

Kusuhara F, Azuwara K, Shiohara H, Otani S (2004) Tests of reinforced concrete interior beam-column joint subassemblage with eccentric beams. In: 13th world conference in earthquake engineering, August 1–6, 2004, paper 185, Vancouver

Lee HJ, Ko JW (2007) Eccentric reinforced concrete beam-column connections subjected to cyclic loading in Principal directions. ACI Struct J 104(4):459–467

Lee JY, Kim JY, Oh GJ (2009) Strength deterioration of reinforced concrete beam-column joints subjected to cyclic loading. Eng Struct 31:2070–2085. https://doi.org/10.1016/j.engstruct.2009.03.009

Leon RT (1990) Shear strength and hysteretic behaviour of interior beam-column joints. ACI Struct J 87(1):3–11

Li B, Wu W, Pan TC (2002) Seismic behavior of nonseismically detailed interior beam-wide column joints—Part 1: experimental results and observed behaviour. ACI Struct J 99(6):791–802

Lima C (2012) Beam-to-column joints in RC frames: capacity models and behaviour under seismic actions. Lap Lambert Academic Publishing. ISBN: 978-3-8484-2227-2

Lima C, Martinelli E, Faella C (2012a) Capacity models for shear strength of exterior joints in RC frames: state-of-the-art and synoptic examination. Bull Earthq Eng 10:967–983. https://doi.org/10.1007/s10518-012-9340-4

Lima C, Martinelli E, Faella C (2012b) Capacity models for shear strength of exterior joints in RC frames: experimental assessment and recalibration. Bull Earthq Eng 10:985–1007. https://doi.org/10.1007/s10518-012-9342-2

Mander JB, Panthaki FD, Kasalanati A (1994) Low cycle fatigue behaviour of reinforcing steel. ASCE J Mater Civ Eng 6(4):453–468. ISSN: 0899-1561/94/0004-0453

Melo J, Varum H, Rossetto T (2015) Cyclic response of RC beam-column joints reinforced with plain bars. Earthq Eng Struct Dynam 44:1351–1371. https://doi.org/10.1002/eqe.2521

M.II.TT. "Italian Ministry of Infrastructure and Transportation" (2008) Norme Tecniche per le Costruzioni (in Italian). Gazzetta Ufficiale n. 29 del 4 febbraio 2008—Suppl. Ordinario n. 30

Miner MA (1945) Cumulative damage in fatigue. J Appl Mech 67:159–164

Palmgren AZ (1924) Die Lebensdauer von Kugellagern. Z des Ver Dtsch Ing (VDI Zeitschrift), 68(14):339–341. ISSN: 0341-7258

Pampanin S, Calvi GM, Moratti M (2002) Seismic behaviour of RC beam-column joints designed for gravity loads. In: 12th European conference on earthquake engineering, Paper 726, London

Paulay T, Priestley MJN (1992) Seismic design of reinforced concrete and masonry buildings. Wiley, New York. ISBN 0-471-54915-0

Shin M, LaFave JM (2004) Seismic performance of reinforced concrete eccentric beam-column connections with floor slabs. ACI Struct J 101(3):403–412

Shiohara H, Zaid S, Otani S (2000) Test of an innovative reinforcing detail for high-performance RC interior beam-column connections subjected to seismic action. Report of University of Tokio, Tokio

Takaine Y, Nagai S, Maruta M (2008) Structural performance of RC beams and beam-column subassemblages using reinforcement with sleeve joints at the end of beams. In: The 14th world conference on earthquake engineering, 12–17 October 2008, Beijing

Teng S, Zhou H (2003) Eccentric reinforced concrete beam-column joints subjected to cyclic loading. ACI Struct J 100(2):139–148

Tsonos AG (2007) Cyclic load behaviour of reinforced concrete beam-column subassemblages of modern structures. ACI Struct J 104(4):468–478

Tsonos AG, Tegos IA, Penelis GG (1992) Seismic resistance of type 2 exterior beam-column joints reinforced with inclined bars. ACI Struct J 89(1):3–12

Verderame GM, Iervolino I, Ricci P (2009) Report on the damages on buildings following the seismic event of 6th of April 2009, V1.20. http://www.reluis.it/doc/pdf/Aquila/Rapporto_fotografico_V1.2.pdf. Accessed 21 March 2018

Wong HF, Kuang JS (2008) Effects of beam-column depth ratio on joint seismic behaviour. In: Proceedings of the institution of civil engineers, structures & buildings, 161(SB2):91–101, Paper 700010. https://doi.org/10.1680/stbu.2008.161.2.91